The success of complex networks at criticality

Victor Hernandez-Urbina* and J. Michael Herrmann
Institute of Perception, Action and Behaviour,
University of Edinburgh. EH8 9AB
United Kingdom.

Tom L. Underwood
School of Physics and Astronomy, SUPA,
University of Edinburgh. EH9 3JZ
United Kingdom.
(Dated: October 24, 2021)

In spiking neural networks an action potential could in principle trigger subsequent spikes in the neighbourhood of the initial neuron. A successful spike is that which trigger subsequent spikes giving rise to cascading behaviour within the system. In this study we introduce a metric to assess the success of spikes emitted by integrate-and-fire neurons arranged in complex topologies and whose collective behaviour is undergoing a phase transition that is identified by neuronal avalanches that become clusters of activation whose distribution of sizes can be approximated by a power-law. In numerical simulations we report that scale-free networks with the small-world property is the structure in which neurons possess more successful spikes. As well, we conclude both analytically and in numerical simulations that fully-connected networks are structures in which neurons perform worse. Additionally, we study how the small-world property affects spiking behaviour and its success in scale-free networks.

I. INTRODUCTION

Cascading behaviour in complex networks refers to a domino effect resulting from the activation of nodes in a network whose internal dynamics are subject to threshold mechanisms and propagation of events (e.g. action potentials, diseases, fads, articles becoming cited, etc.). In the context of cascading behaviour, the success of a node refers to its capacity (once it becomes active as a result of its internal dynamics) to trigger subsequent activations in its neighbourhood. Intuitively, network structure plays a major role on determining how activity spreads through a system. In this respect, the discovery of topological features such as the small-world property and the scale-invariance of the degree distribution in many real-world networks provided a new perspective in which to analyze cascading activity.

The study of complex networks took off when it was observed that the essence of real-world networks cannot be captured by the random network model introduced by Erdös and Renyi [1] nor by regular structures such as lattices. The Watts and Strogatz model [2] was proposed to describe a class of networks that lie halfway between randomness and regularity. This class of networks are characterized by a small average shortest path length (a feature observed in random networks) and an average clustering coefficient significantly larger than expected by chance (a feature observed in regular lattices). Taken together, these properties offer a structural benefit to the

processes taking place within the network, such as optimal information transmission that results from speeding up the communication among otherwise distant nodes. A term that summarizes the presence of these two properties is that of the *small-world property*. Networks that exhibit the small-world property are so diverse and can be found in social, technological and biological contexts, to name a few [3].

Scale-invariance in the distribution of the node degrees of a network is a phenomenon observed in real-world networks. Networks that exhibit this particular feature are known as *scale-free networks*. In this type of networks the probability $P(k)$ that a node connects to k other nodes follows a power-law $P(k) \sim k^{-\gamma}$ [4]. It implies the existence of many poorly connected nodes coexisting with very few but not negligible massively connected nodes *hubs*. Scale-invariant degree distribution and the small-world property are by no means exclusive and in fact many scale-invariant networks are also small-world.

When it comes to the dynamics of a system comprising numerous interconnected elements interacting non-linearly, a considerable number of studies have been dedicated to the occurrence of power-law behaviour and its relationship to the notion of phase transitions, $1/f^{\alpha}$ noise and *self-organized criticality* (SOC) [5] that results from the collective dynamics of the threshold units comprising a system.

The concept of SOC, has been suggested to explain the dynamics of phenomena as diverse as plate tectonics [6], piles of granular matter [7], forest fires [8], neuronal avalanches [9] (see below), and mass extinctions [10], among several others. Moreover, SOC implies the existence of a critical point that becomes an attractor in

―――――――
* j.v.hernandez-urbina@ed.ac.uk

the collective dynamics of a system. Such a critical point or regime denotes a state of the system in which the collective dynamics are undergoing a phase transition. As such, it represents the boundary between two different states of the system (e.g. order and chaos) and it is identified by the presence of power laws in the distribution of events, the divergence of the correlation length, among others [5].

In the context of brain networks, the presence of neuronal avalanches has been observed as the result of spontaneous activity in local field potentials of cultured slices of rat cortex [11], and in the superficial cortical layers of awake, resting primates [12]. As the name suggests, neuronal avalanches are an example of cascading behaviour triggered by spiking in groups of neurons. The observed avalanches are stable and repeatable spatiotemporal patterns of activity [13], which might relate them to memory mechanisms inside the brain.

In models of neuronal avalanches, it has been reported that the distribution of their sizes as well as the distribution of their durations can be approximated by a power law with very precise exponents in the thermodynamic limit as well as scaling relationships among system sizes and exponents [9, 14]. As mentioned earlier, this phenomenon has also been reported in real brain tissue (although with finite-size effects) [11]. Power-law behaviour in the dynamics of neuronal avalanches relate this biological process to the notion of SOC described above.

Critical dynamics of brain networks have been studied thoroughly in artificial models, and it has been found that the critical regime implies several computational benefits for the system, namely: optimal information transmission and maximum dynamic range [15], maximum information storage [16, 17], stability of information transmission [18], among others. Hence the criticality hypothesis for brain dynamics, which states that neural networks operate at the *edge of chaos*, that is, at the critical point in a phase transition between total randomness and boring order [19].

In this paper we study the success of integrate-and-fire nodes in terms of their capacity to trigger subsequent spikes in their neighbourhood once they become active, and thus giving rise to cascading activity. We study this local performance in topologies such as fully-connected, random, and scale-free networks with varying amounts of the small-world property when the systems are at the critical state of their collective dynamics.

II. MODEL

A. The Eurich model

The model consists of N non-leaky integrate-and-fire nodes and was formulated for fully-connected networks [9]. This model exhibits critical dynamics in the collective behaviour of the units comprising the system. This fact is identified by the presence of neuronal avalanches, whose size and durations can be approximated by a power law. In analytical examinations, the exponents derived for such distributions are $\gamma = -3/2$ and $\delta = -2$ for avalanches sizes and durations respectively, in the thermodynamic limit of fully-connected networks [9, 14]. Here we will extend such a model by considering also heterogeneous directed networks.

In the model, each node j is characterised by a continuous variable known as the membrane potential h, which is updated in discrete time according to the equation:

$$h_j(t+1) = h_j(t) + \sum_{i=1}^{N} A_{ij} w_{ij} s_i(t) + I_{ext} \qquad (1)$$

where A denotes the asymmetric adjacency matrix with entries $A_{ij} = 1$ if node i sends and edge to node j, and $A_{ij} = 0$ otherwise; w_{ij} denotes the synaptic strength from node i to node j; $s_i(t) \in \{1, 0\}$ represents the state of node i (active or quiescent, respectively) at time t; and I_{ext} denotes external input which is supplied to a node depending on the state of the system at time t. This mechanism of external driving works as follows: if there is no activity at time t, then a node is chosen uniformly at random and its membrane potential is increased by a fixed amount through the variable I_{ext}. If $h_i(t)$ exceeds the threshold θ, which in simulations is set to unity, then node i emits a spike, which changes the state of this node to active ($s_i(t) = 1$) and propagates its activity through its synaptic output. Afterwards, the node is reset, ie. $h_i(t+1) = 0$.

The coupling strength w_{ij} for every node i sending an edge to node j is set according to the equation $w_{ij} = \alpha / \langle e \rangle$ where α is the control parameter of the model and $\langle e \rangle$ denotes the mean degree of the network; which is the same for all the network structures considered (see below), except for fully-connected networks, in which case mean connectivity is $(N-1)$.

In the first stages of our experiments we let the parameter α take values in the interval $(0, 1)$, and then we measure the deviation from the best power-law fit to the distribution of avalanche sizes (see Sect. II D for details). The values of α for which the deviation is at its minimum are those who lead the system to the critical state, and define the critical interval. In a second stage of our experiments we re-start the system considering only values of α taking uniformly at random from the critical interval. The critical interval varies for different types of networks and system sizes.

As mentioned above, in this work we consider different types of network structures as well as system sizes. The topologies considered are:

 i. fully connected,

 ii. random,

 iii. scale-free with *low* mean clustering coefficient (CC) and power-law in the out-degree distribution,

iv. scale-free with *high* mean CC and power-law in out-degree distribution,

v. scale-free with *low* mean CC and power-law in in-degree distribution,

vi. scale-free with *high* mean CC and power-law in in-degree distribution.

System sizes for each of these classes of networks are: 128, 256, 512, and 1,024. We should point out an important aspect of the networks that we consider. For the case of random and scale-free networks the number of edges is the same for each system size, which results in the same average connectivity for these types of networks. Thus, the topology results from a particular permutation of the edges. However, this edge permutation is not arbitrary, but results from a particular algorithm depending on the structure that we want to obtain. In the case of random networks the mechanism, by which we permutate such edges, is given by the Erdös-Renyi model [20], whereas for scale-free networks with tuneable clustering we follow the ideas in Ref. [21], in which the authors present an extended version of the *BA model* [4], in which a large mean clustering coefficient is achieved for scale-free networks by adding a triangle-formation step to the preferential attachment algorithm. This algorithm produces scale-free networks whose mean clustering coefficients match better the observations in real-world networks.

In the following section we describe the structural differences of networks whose in-degree distribution follows a power-law, and networks whose out-degree distribution follows a power-law.

B. Broadcasting hubs and absorbing hubs

Scale-free networks are characterized by a power-law approximation of their degree distribution [4]. In the case of directed networks, there are two degree distributions, one corresponding to the out-degrees of nodes and another one for the in-degree of nodes. In general, real-world networks are directed, and very often both their degree distributions can be approximated by a power-law (e.g. the World Wide Web [20]), or at least one of them (e.g. citation networks [20]). In either case, the presence of a long-tail in the *out-degree* distribution of a network implies the existence of *broadcasting hubs*, that is, nodes that have massive outgoing connections compared with other nodes in the system. On the contrary, the presence of a long-tail in the *in-degree distribution* implies the existence of *absorbing hubs*. Here, we are interested in analyzing how collective dynamics develop for the case of networks with broadcasting hubs and for networks with absorbing hubs. In the following, scale-free networks with absorbing hubs will be labeled as *in-degree scale-free networks*, whereas those that contain broadcasting hubs will be termed *out-degree scale-free networks*.

As mentioned in the introduction, the small-world property is not a binary one, and as such, there exist degrees of what we would call *small-world-ness*. All the scale-free networks considered possess the small-world property up to a certain amount. In our model we consider two levels of mean clustering for scale-free networks (*low* and *high*) by tuning a simple parameter [21]. The process of tuning the mean clustering coefficient in these types of networks has an immediate effect on the degree of small-world-ness of such networks. Scale-free networks with low mean clustering coefficient possess a low degree of small-world-ness when compared against scale-free networks with high mean clustering coefficient. In this study, we inquire on the effects on criticality for different degrees of small-world-ness.

C. Node success

We introduce a local measure of the performance of a node during simulation time. The node success of node i at time t is the fraction of *out-neighbors* of this node that become active at time $t + 1$ when node i spikes at time t, in other words:

$$\varphi_i(t) = \frac{\sum_{j=1}^{N} A_{ij} s_j(t+1)}{\sum_{j=1}^{N} A_{ij}} \qquad (2)$$

where A is the adjacency matrix, and $s_j(t+1)$ the state of node j at time $t + 1$.

Thus, node success measures the performance of an individual spike in terms of the subsequent spikes triggered by such initial activation, which occur within the out-neighborhood of a given node. In contrast to many other popular network statistics (e.g. degree distribution, branching ratio [11], etc.) node success is a local measure of performance.

We consider two different averages of this measure. First, the *mean node success per node* which results from considering only the times in which a node spikes and then averaging its node success at each of these times. Second, the *mean node success per time step* which results from averaging the node successes of all nodes in the system at a particular time step.

D. Numerical implementation

When starting simulations, all membrane potentials are initialised at random taking values in the interval $(0, 1)$, whereas all states are set to inactive. By means of external driving, activity inside the system in the form of neuronal avalanches is guaranteed to occur. However, avalanche sizes and their durations will not always be the same nor can they be predicted.

Both the relaxation time towards the critical state as well as the sampling time needed to assess criticality depend on the system size. For networks consisting of 128 nodes we allow critical dynamics to set in for one million

time steps according to the Eurich model [9]; for networks of 256 nodes we allow critical dynamics to set in for two million time steps, for networks comprising 512 we allow for three million time steps, and finally for networks of 1,024 elements the dynamics run for four million time steps. This selection of times is appropriate for large events (that is avalanches that extend to the whole network) to take place during simulation time. With this in mind, we expect to have small events (i.e. small avalanches) coexisting with large events (i.e. avalanches that span the whole system). An inspection of the distribution of avalanche sizes after this driving stage shows a distribution that can be approximated by a power law with a cut-off due to the finite nature of the system (see Sect. III A). The power-law approximation of such a distribution implies that the system is in the critical regime with very frequent small events coexisting with rare but not negligible large events.

We assess the quality of such a power law through the mean-squared deviation $\Delta\gamma$ from the best-matching power law with exponent γ obtained through regression in log-log scales. Our choice of using this method is due to its simplicity and justified by the asymptotic unbiasedness of the estimation. When this error function is at its minimum, that is, when the data is best approximated by a power-law distribution with exponent γ, is when the system is at the critical state.

For our experiments we consider 50 different networks per class (*ii* to *vi* described above) and system size for the sake of statistical robustness. In the case of fully-connected networks, as there exists only one fully-connected network of size N, randomness is introduced in the seed of the pseudorandom number generator used in our code for each realization of the experiment rather than in the structure as for the other network classes considered. Experiments were carried out in the EDDIE computer cluster of the University of Edinburgh.

III. RESULTS

A. Avalanche size distribution follows a power-law

As mentioned in Sect. II D, we assess the quality of the power-law approximation to the distribution of avalanche sizes by estimating the deviation from the best power-law fit. When such an error function reaches a minimum value of less than or equal to 0.05, we consider the event-size distribution as well approximated by a power-law and conclude that the system is in a critical state. Fig. 1a shows the power-law fitting error as a function of simulation time for the distribution of avalanche sizes for scale-free and random networks of size $N = 512$. This figure shows the deviation, $\Delta\gamma$, of our data from the best matching power law with exponent γ. In this figure, we present mean values and standard deviations of $\Delta\gamma$ obtained from the realizations of our experiments. Fig. 1b shows the distribution of avalanches sizes for all scale-free
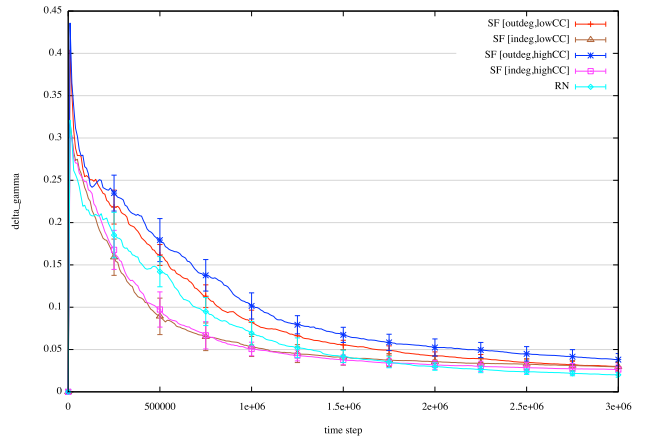
(a) Power-law fitting deviation per time step
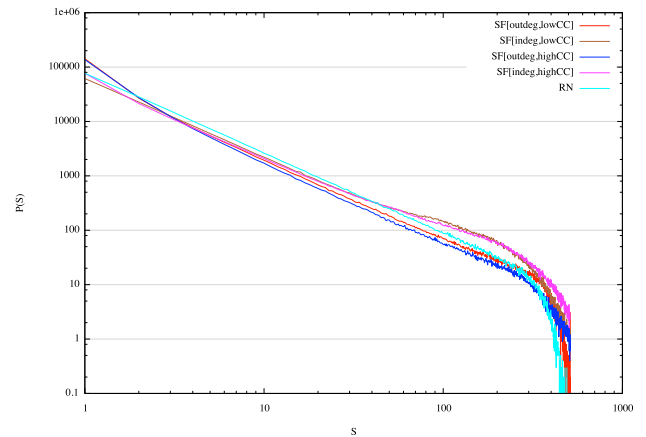
(b) Log-log plot of distribution of avalanche sizes S

FIG. 1: Deviation from power-law matching per time step for a network of size $N = 512$. The minimum error reached at time step 3×10^6 corresponds to the critical regime identified by a power law distribution of avalanche sizes. We show the averaged value of all realizations, but we do not present error bars in Fig. 1b in order to make its presentation more accessible.

and random networks of size $N = 512$ at criticality (ie. when $\Delta\gamma \le 0.05$ around time step 3×10^6 in Fig. 1a). We show the averaged value of all realisations, but we do not present error bars in Fig. 1b in order to make its presentation more accessible. Although we show the distribution of avalanche sizes and the deviation from the best matching power-law for a particular system size, all system sizes exhibit a similar behaviour.

Moreover, following Ref. [22] we inspect the value of the largest eigenvalue of the matrices W associated to each network and whose entries w_{ij} denote the synaptic weight between node i and j. The authors in Ref. [22] observe that the largest eigenvalue of the weight matrix governs the dynamics of the system. Through an analytical examination, it is reported that when the largest eigenvalue equals unity the system is at the critical state.
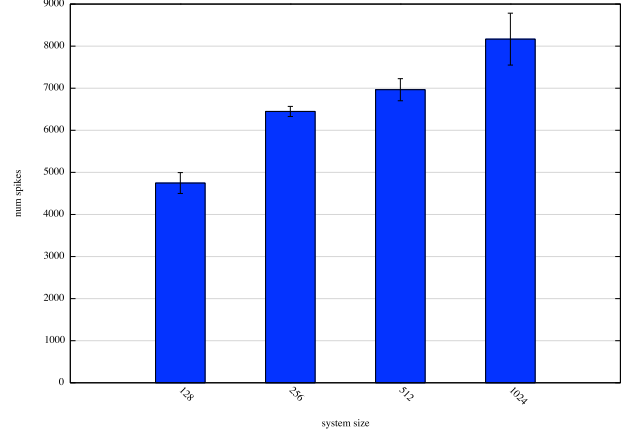
Type	Subtype	Size	Λ
Out-degree scale-free	Low Mean CC	128	0.906 ± 0.029
		256	0.9 ± 0.02
		512	0.95 ± 0.01
		1,024	0.97 ± 0.008
	High Mean CC	128	0.89 ± 0.04
		256	0.91 ± 0.03
		512	0.91 ± 0.01
		1,024	0.94 ± 0.01
In-degree scale-free	Low Mean CC	128	0.98 ± 0.02
		256	0.99 ± 0.01
		512	1.0006 ± 0.006
		1,024	1.001 ± 0.004
	High Mean CC	128	0.96 ± 0.02
		256	0.99 ± 0.02
		512	1.002 ± 0.014
		1,024	1.01 ± 0.017
Random		128	0.92 ± 0.012
		256	0.99 ± 0.022
		512	0.97 ± 0.001
		1,024	0.98 ± 0.005
Fully-connected		128	0.91 ± 0.034
		256	0.93 ± 0.0006
		512	0.95 ± 0.001
		1,024	0.98 ± 0.0005

TABLE I: Largest eigenvalue Λ of matrix W of synaptic weights. It has been found analytically that $\Lambda = 1$ is associated with a system at criticality [22]. The synaptic weight matrices of our networks have $\Lambda \approx 1$ due to finite-size effect. (We present mean values and standard deviations.)
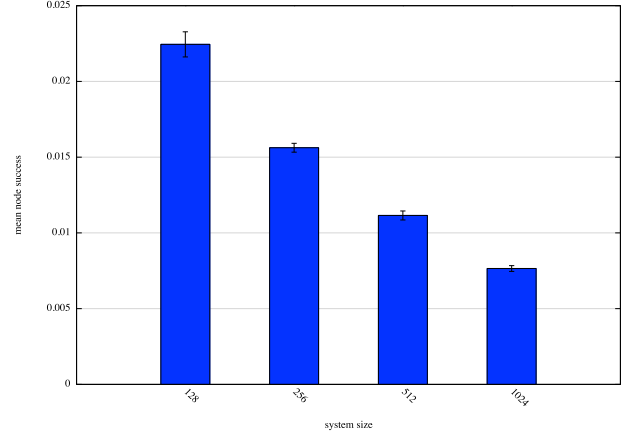

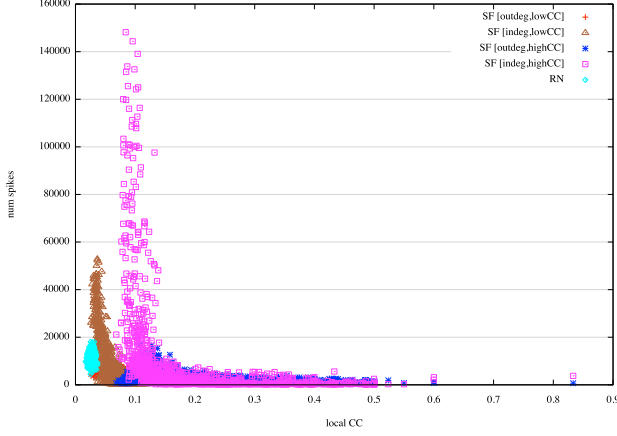(a) Total number of spikes

(b) Total mean node success

FIG. 2: Average number of spikes emitted by fully-connected networks per system size and their mean success. (Error bars denote standard deviations.)

In Table I we report the value of the largest eigenvalue Λ of the weight matrices associated to our networks. In our experiments the critical state is not only identified by the power-law distribution of avalanche sizes (Fig. 1) but also by the value close to unity of Λ. Due to finite size effects this value is not exactly unity but close to it.

B. Small-world property boosts network activity

The small-world property affects the rate of firing of nodes comprising a network. Fully-connected networks are structures in which all nodes exhibit a similar firing rate, giving rise to a well defined mean and variance (see Fig. 2a) unlike scale-free networks in which the variance of the firing rate seemingly diverges, and thus its mean cannot characterize the network activity (not shown here). In fact, this latter type of structure contains nodes whose firing rate can far exceed the firing rate in fully-connected networks (see Fig. 3a).

Fig. 2a shows the average of the total number of spikes over all nodes in fully-connected networks for all system sizes considered. In contrast, we will show that nodes in heterogeneous topologies can perform better; in this case, scale-free networks possess nodes with higher firing rates than random networks. It is worth mentioning that this behaviour is verified in all system sizes considered.

We pose several questions regarding the relationship between network structure and dynamics. The first is: are the nodes with higher local CC those that spike more often, that is, do better-clustered nodes fire more? Surprisingly, nodes with low local CC exhibit a larger spiking rate than more clustered nodes. Fig. 3a shows this behaviour for networks of size $N = 1,024$. Here we show not only that low locally clustered nodes fire more but also that in in-degree scale-free networks nodes can fire more than in any other type of structure.
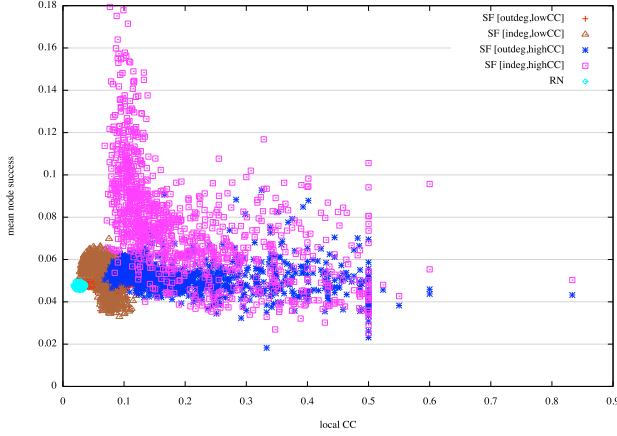
A question that arises at this point is the following: are those low locally clustered nodes who spike so frequently
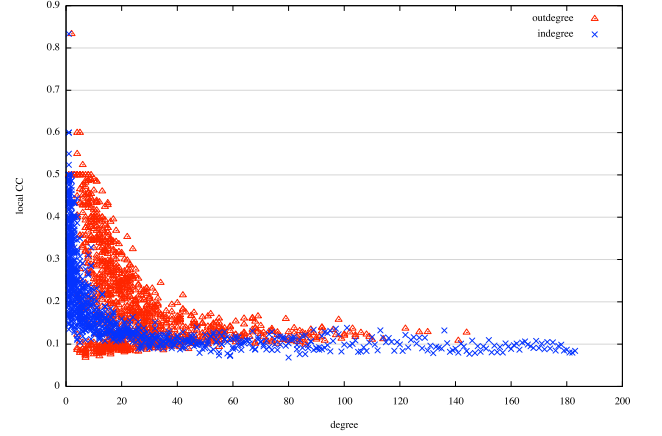
(a) Total number of spikes
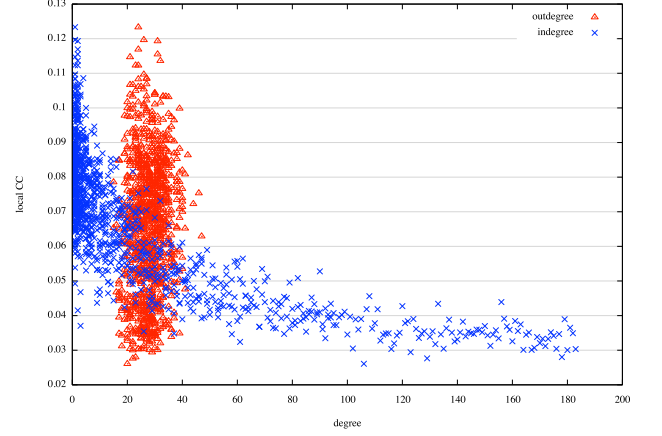
(b) Total mean node success

FIG. 3: Total number of spikes and mean node success per local CC for heterogeneous topologies of size $N = 1,024$. Low clustered nodes are responsible for spiking more frequent in scale-free networks. Their spikes tend to be more successful as well.

(a) Low mean CC

(b) High mean CC

FIG. 4: In scale-free networks well connected nodes are less clustered. Here we show for size $N = 1,024$ and in-degree scale-free nets with the two levels of mean CC (low and high). For the case of out-degree scale-free nets, degree distributions are switched so that out-degree becomes in-degree and vice versa.

in in-degree scale-free networks the absorbing hubs or any other type of node? Taking a look at network topology, we verify that indeed hubs (either absorbers or broadcasters) are in general low locally clustered. In Fig. 4 we present for scale-free networks of size $N = 1,024$ and two levels of mean CC (low and high) the relationship between in-degree/out-degree and local CC. The more a node is in-connected the lower its local CC (likewise when reversing the direction of edges, which yields broadcasting hubs).

Then, we verify that better-connected nodes possess higher firing rate than any other type of node. In Fig. 5 we present how the two different degree distributions (in and out) are related to spiking activity in scale-free networks. Fig. 5a shows this for low mean clustered scale-free networks, whereas Fig. 5b shows it for high mean clustered networks. For the case of out-degree scale-free networks, that is, networks that possess broadcasting

hubs we do not observe any correlation between node out-degree and firing activity. This occurs in out-degree scale-free networks with low and high mean CC, and across all system sizes. However, for the case of in-degree scale-free networks, that is, networks that include absorbing hubs, we observe a positive correlation between node in-degree and spiking. This behaviour occurs in all system sizes. Interestingly, the behaviour of in-degree scale-free networks with low mean CC differ from the behaviour of the same type of network with high mean CC. Both exhibit a positive correlation between in-degree and total number of spikes, nevertheless low mean clustered networks exhibit a linear trend, whereas high mean clustered ones exhibit a non-linear trend. This suggests that as a network becomes more clustered (and more *small-worldly*) the activity of their nodes exhibit a more quadratic dependency of the node's in-degree. We do not
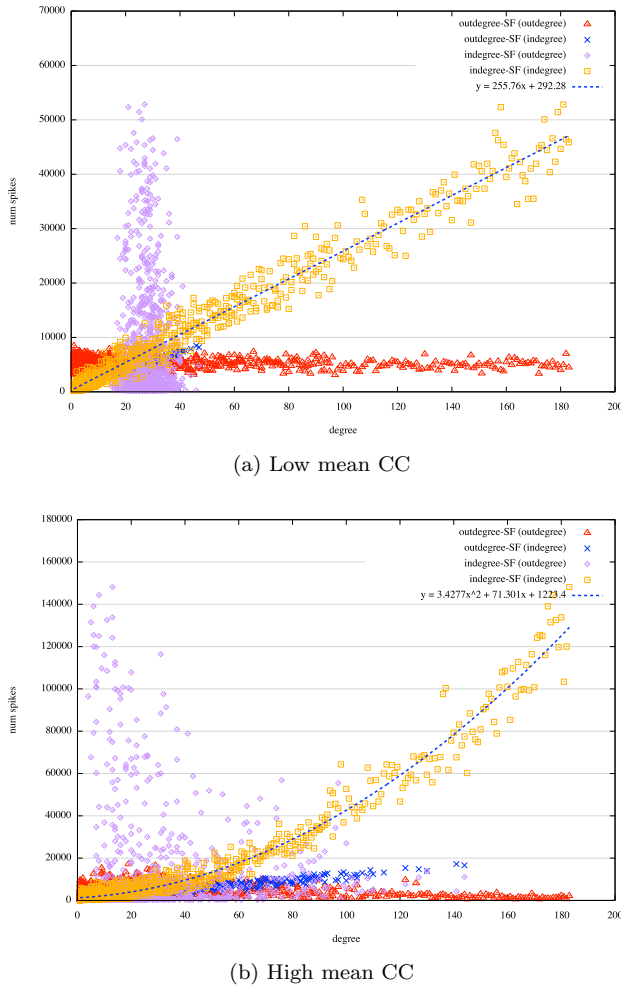
(a) Low mean CC

(b) High mean CC

FIG. 5: In in-degree scale-free nets the absorbing hubs spike more than any other type of node and their in-degree is correlated with the amount of spikes fired. For networks with higher mean CC this correlation is quadratic. We show this behaviour for a network of size $N = 1,024$.

explore this hypothesis in the present work, but it is the direction of future research.

At first, the observation of a positive correlation between spiking and node in-degree would seem very obvious, in the sense that nodes with high in-degree are driven beyond threshold frequently by the action of their in-neighbors. However a high in-degree cannot explain completely the high firing rate of this type of nodes, because this would also predict that nodes in fully-connected networks would possess a high firing rate, which is not the case (see Fig. 2a). What is happening in fully-connected networks that prevents nodes from firing as much as the other heterogeneous structures considered even when these nodes are massively connected? We suggest that an obstructing behaviour is occurring in this globally-coupled structure. We name this phenomenon *spike jamming* and we will discuss it in detail in Sect. III D.

Random networks behave somehow similarly to scale-free networks in the sense that there is a positive correlation between node in-degree and spiking, but not between this latter and node out-degree. However, this type of structure does not reach the same amount of spiking per node as scale-free networks due to the random nature of their connectivity (not shown here). Thus, the presence of hubs account for the high firing rate in heterogeneous structures.

Another question that arises at this point is the following. Does a high in-degree in scale-free networks account by itself for a high spiking activity? Or is it the joint action of in- and out-degree that explain this particular behaviour? In other words, could this high firing rate be explained by a specific configuration of in- and out-degree? To explore this question we considered the ratio of in-degree to out-degree per node, which for a node i is given by:

$$\rho_i = \frac{\sum_{k=1}^{N} A_{ki}}{\sum_{j=1}^{N} A_{ij}} \qquad (3)$$

where the numerator is the in-degree of node i, and the denominator is its out-degree. The quantity ρ is equal to unity when a node has the same number of incoming and outgoing connections. In fully-connected networks all nodes possess this property. If $\rho_i > 1$, then the in-degree of node i is larger than its out-degree, and $\rho_i < 1$ when the opposite occurs.

From fully-connected networks we have learned that homogeneity in node degree, that is, $\rho = 1$ for every node, is not a property suitable for spiking. Moreover, we verify this fact in heterogeneous structures where nodes with $\rho \gg 1$ fire more than any other nodes. Fig. 6a shows this particular behaviour. There we present how spiking is improved as ρ grows larger than unity. The solid black line at left of Fig. 6a marks the point where $\rho = 1$, ie. where in-degree equals out-degree. For all heterogeneous structures considered (excluding random networks) a larger in-degree than out-degree correlates with higher firing rate.

In summary, in fully-connected networks nodes fire less than in any other topology. This is explained by the homogeneity of the nodes comprising the network, which give rise to the phenomenon of spike jamming. In heterogeneous topologies, scale-free networks fire more than random networks, and the firing activity is improved by the presence of absorbing hubs and high mean CC, which implies a larger degree of small-world-ness. However, for this to happen absorbing hubs must possess the right amount of outgoing connections which is represented by $\rho \gg 1$.
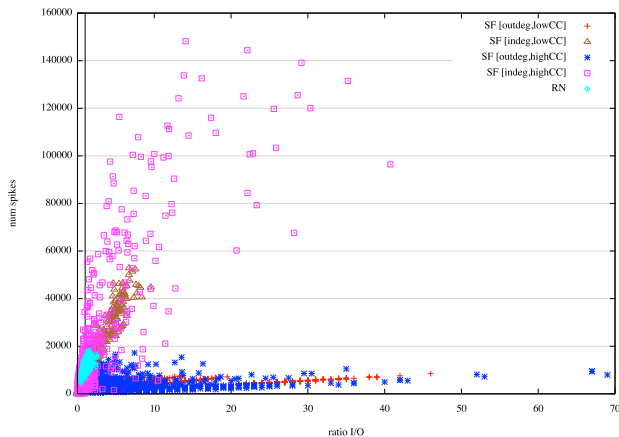
(a) Total number of spikes
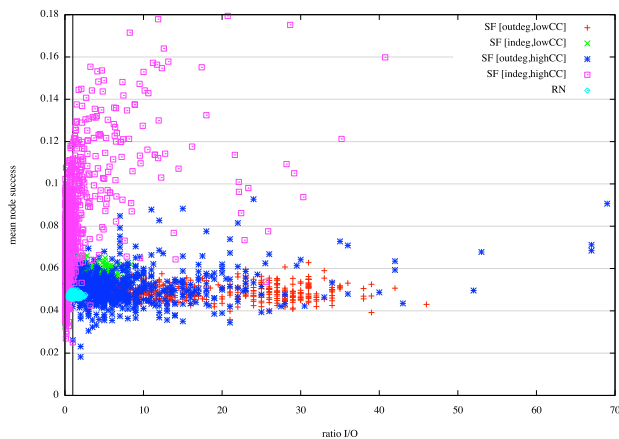
(b) Total mean node success

FIG. 6: Total number of spikes and their success per ratio in-degree/out-degree for heterogeneous nets of size $N = 1,024$. The solid line at the left lies at $\rho = 1$ where in-degree equals out-degree. An equal number of incoming and outgoing connections cannot account for higher spike rate and spike success.

C. Scale-free topologies comprise more successful nodes

Spiking is not all that matters, since we should also consider the fate of a spike that has just been emitted. Here, we consider a *successful spike* one that triggers subsequent spikes from the nodes in the out-neighborhood of the node where the initial spike originated. As we are interested in the propagation of activity within the system, we would like to observe the sustained activation of nodes in subsequent time steps. This is where the notion of the *branching ratio* comes to hand. The branching ratio σ is defined as the ratio of descendants that become active at time $t + 1$ to ancestors that were active at time t. The quantity σ has been used to characterize the critical state of a system [11] and to identify the regimes surrounding such a state. When $\sigma < 1$ the system is sub-

critical and activity dies out quickly, when this value is above unity, the system is supercritical and activity gets amplified pathologically at each time step. In between these two states lies the critical state in which activity is sustained until finite-size effects take place, during this regime σ is equal to unity for a prolonged period of time.

Recall that in Sect. II C we defined the success of any give node i as the fraction of out-neighbors that become active at time $t + 1$ when node i spiked at time t. This quantity is similar to the branching ratio σ in the sense that it estimates the amount of activity sustained in subsequent time steps. However, unlike σ our measure of node success is a *local* estimation of performance, which has more natural implications in the context of neuronal networks, in which a neuron does not have access to global metrics regarding the structure of the network.

As mentioned above, spiking does not imply success, and node success as defined above is intimately related to the notion of criticality. Here we repeat the same questions that we considered in the previous section, namely, how successful are nodes with high local CC? how successful are hubs? and finally, how network structure affect node success?

For scale-free networks, nodes with low local CC are the most successful nodes. This behaviour is more evident in in-degree scale-free networks with high mean CC (see Fig. 3b). These low local CC nodes are the hubs, however unlike the firing activity, mean node success per node does not exhibit a very clear correlation between in- or out-degree and success (see Fig. 6b). Finally, random networks do not exhibit any particular pattern regarding the success of their nodes.

Which is the most successful topology? In other words, what is the structure that maximises the success per node? To answer this question we estimated the mean node success of the system per time step (see Sect. II C) for all the topologies considered.

For all system sizes we observe that fully-connected networks are the type of structure that performs worst (see Fig. 2b), followed by random networks. For the case of scale-free networks, in-degree scale-free networks with high mean CC are the most successful topologies. Second in place are in-degree scale-free networks with low mean CC, followed by out-degree scale-free networks with high and low mean CC, respectively. Thus, absorbing hubs in a scale-free structure allow for more node success per node if accompanied by a high degree of small-world-ness.

Recall that the scale-free and random topologies have the same number of edges. Therefore, in-degree scale-free-ness with high mean CC is the permutation of edges that maximises node success. Fig. 7 shows the aforementioned behaviour for networks of size $N = 1,024$, the same is observed in all the other system sizes considered.

Moreover, the value of the mean node success per time step is upper bounded. For a system to remain in the critical regime the mean node success must remain below a certain value. In other words, a high mean node success is related to the supercritical regime in which nodes fire
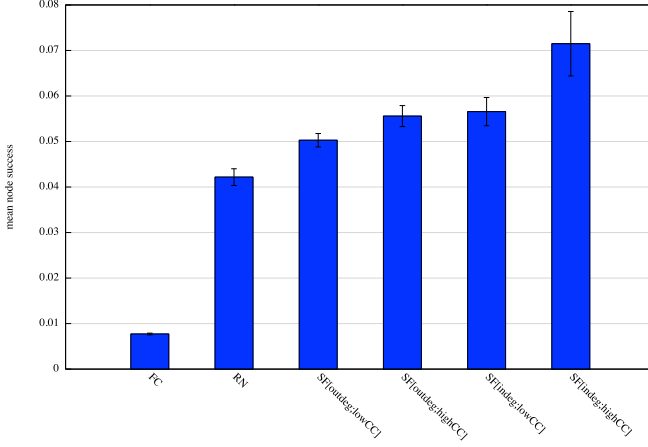
FIG. 7: Mean node success for scale-free and random networks of size $N = 1,024$. In-degree scale-free networks with high mean CC possess more successful nodes than any other topology considered. (Error bars denote standard deviations.)

constantly (not shown here); so that, if we were interested in maximizing the value of the mean node success we would have to leave the critical regime. Additionally, we report that the upper bound of the total mean node success at criticality decreases as the system size grows. An example of this is shown in Fig. 2b where the maximum value of node success for fully-connected topologies decrease with system size. Although not shown here, this phenomenon is observed in all other topologies and systems sizes.

D. Upper bound of mean node success for fully-connected nets

As mentioned in the previous section, fully-connected networks perform worst as measured by the mean node success per time step. In this section we derive an analytical expression for the upper bound of this metric for globally-coupled structures.

Recall that $h_i(t)$ denotes the membrane potential of node i at time step t, and that $\theta > 0$ denotes the threshold membrane potential required to trigger a spike in a node: node i will spike at t when $h_i(t) \geq \theta$. At $t = 0$ the membrane potentials take values $h_i(0) < \theta$ for all i. These potentials are then *driven externally* each time step until the membrane potential of one node is taken above the threshold membrane potential - triggering an avalanche. During an avalanche the membrane potentials evolve as follows:

$$h_i(t+1) = \begin{cases} 0 & \text{if } h_i(t) \geq \theta \\ h_i(t) + \sum_{j \in \mathcal{I}_i} w_{ij} s_j(t) & \text{otherwise,} \end{cases} \quad (4)$$

where $\mathcal{I}_i$ denotes the set of in-neighbors of i, and recall that w_{ij} describes the coupling between nodes i and j, and that $s_j(t) = 1$ if node j spikes at t and 0 otherwise, i.e.

$$s_j(t) = \begin{cases} 1 & \text{if } h_j(t) \geq \theta \\ 0 & \text{otherwise.} \end{cases} \quad (5)$$

Note that the membrane potentials are *not* driven during the avalanche. The avalanche ends when there are no more spiking nodes. Afterwards, the membrane potentials are then driven again each time step until another avalanche is triggered. This process is repeated until the simulation ends.

In a fully connected network each node has $(N-1)$ out-neighbors, where N denotes the number of nodes in the network. Specifically, the out-neighbors of node i are all the nodes j such that $j \neq i$. Recall that the node success $\varphi_i(t)$ of node i at time step t is defined as the fraction of out-neighbors of i which spike at time step $t+1$, given that i spikes at t. Therefore, if i spikes at t[23], Eqn. (2) becomes

$$\varphi_i(t) = \frac{S(t+1)}{N-1} \quad (6)$$

in a fully connected network, where $S(t)$ denotes the number of nodes which spike at time step t. Note that the right-hand side of the above expression is independent of i. This reflects the fact that $\varphi_i(t)$ is identical for all nodes i which spike at t. For this reason we will henceforth omit the subscript i, and deal only with the quantity $\varphi(t)$, the node success of *any* node which spikes at t. This observation is only valid for fully-connected networks in which all nodes receive connections from each other and send connections likewise.

Consider the mean node success for nodes which spike during any period of τ time steps. Since $S(t)$ nodes spike at t, this is given by

$$\langle \varphi \rangle = \frac{1}{\mathcal{S}} \sum_{t=1}^{\tau} S(t) \varphi(t), \quad (7)$$

where without loss of generality we have chosen the τ timsteps to be $t = 1, 2, \ldots, \tau$, and

$$\mathcal{S} \equiv \sum_{t=1}^{\tau} S(t) \quad (8)$$

is the total number of spikes which occur during this period. A crucial aspect of the dynamics described above is that $h_i(t+1) = 0$ if node i spikes at time t. It is therefore impossible for node i to spike on two adjacent time steps – after spiking, the membrane potential of node i is *frozen* (due to refractoriness) to be zero for a single time step, during which time it cannot 'accumulate activity' from spiking in-neighbors in the manner described

by Eqn. (4). This constraint can be expressed mathematically as

$$s_i(t) + s_i(t+1) \leq 1 \quad \text{for all } i, t, \quad (9)$$

and leads to the following theorem:

Theorem 1. $\langle \varphi \rangle$ *has an upper bound of*

$$\langle \varphi \rangle_{max} = \frac{N}{2(N-1)} \quad (10)$$

in the limit $\tau \to \infty$. This upper bound is realised when $S(t) = N/2$ for all $t > 1$.

Proof: Substituting Eqn. (6) into Eqn. (7) gives

$$\langle \varphi \rangle = \frac{1}{\mathcal{S}(N-1)} \sum_{t=1}^{\tau} S(t)S(t+1). \quad (11)$$

Defining the quantity

$$\tilde{S}(t) \equiv S(t)/\sqrt{\mathcal{S}}, \quad (12)$$

Eqn. (11) can be expressed as

$$\langle \varphi \rangle = \frac{1}{(N-1)} \sum_{t=1}^{\tau} \tilde{S}(t)\tilde{S}(t+1). \quad (13)$$

Now, taking the summation of Eqn. (9) over all nodes i yields [24]

$$S(t) + S(t+1) \leq N \quad \text{for all } t \quad (14)$$

after noting that

$$S(t) = \sum_i s_i(t). \quad (15)$$

Subtracting $S(t+1)$ from both sides of Eqn. (14) and then multiplying throughout by $S(t+1)$ yields

$$S(t)S(t+1) \leq S(t+1)\big[N - S(t+1)\big] \quad \text{for all } t, \quad (16)$$

which can be expressed as

$$\tilde{S}(t)\tilde{S}(t+1) \leq \tilde{S}(t+1)\left[\frac{N}{\sqrt{\mathcal{S}}} - \tilde{S}(t+1)\right] \quad \text{for all } t \quad (17)$$

after dividing both sides by $\mathcal{S}$. [25] The right-hand side of the above inequality, which we denote as

$$\xi(t+1) \equiv \tilde{S}(t+1)\left[\frac{N}{\sqrt{\mathcal{S}}} - \tilde{S}(t+1)\right], \quad (18)$$

is hence an upper bound for term t on the right-hand side of Eqn. (13). Therefore we can write

$$\langle \varphi \rangle \leq \frac{1}{(N-1)} \sum_{t=1}^{\tau} \xi(t+1). \quad (19)$$

Now, $\xi(t+1)$ is maximised when $\tilde{S}(t+1) = N/(2\sqrt{\mathcal{S}})$. Therefore $\tilde{S}(t+1) = N/(2\sqrt{\mathcal{S}})$ for $t = 1, 2, \ldots, \tau$ provides an upper bound for $\langle \varphi \rangle$, which, from substituting the aforementioned $\tilde{S}(t+1)$ into into Eqns. (18) and (19), can be shown to be

$$\langle \varphi \rangle_{\text{max}} = \frac{1}{(N-1)}\left(\frac{N}{2}\right)^2 \frac{\tau}{\mathcal{S}}. \quad (20)$$

However, from Eqn. (12), $\tilde{S}(t+1) = N/(2\sqrt{\mathcal{S}})$ for $t = 1, 2, \ldots, \tau$ corresponds to $S(t+1) = N/2$ for $t = 1, 2, \ldots, \tau$, and hence from Eqn. (8) also corresponds to

$$\mathcal{S} = S(1) + \sum_{t=2}^{\tau} S(t) = S(1) + (\tau-1)N/2. \quad (21)$$

Substituting this into Eqn. (20) gives

$$\langle \varphi \rangle_{\text{max}} = \frac{1}{(N-1)}\left(\frac{N}{2}\right)^2 \frac{\tau}{S(1) + (\tau-1)N/2}. \quad (22)$$

We emphasise that this is realised when $S(t+1) = N/2$ for $t = 1, 2, \ldots, \tau$, or equivalently, when $S(t) = N/2$ for $t = 2, 3, \ldots, \tau + 1$. Noting that $S(1)$ cannot exceed N, Theorem 1 results when the limit $\tau \to \infty$ is taken. ∎

Some remarks are due with regards to Theorem 1. Firstly, $\langle \varphi \rangle$ as $\tau \to \infty$, which we henceforth refer to simply as $\langle \varphi \rangle$, describes the mean node success over all nodes over all time.

Secondly, Theorem 1 applies in a very general way to fully-connected networks, in the sense that for the purpose of proving the theorem we have made no assumptions regarding how the system is driven between avalanches, or the initial values of the membrane potentials. Furthermore, we have made no assumptions regarding the specific values of θ or w_{ij}.

Thirdly, since Theorem 1 pertains to a fully-connected network, it follows that any network with $\langle \varphi \rangle > \langle \varphi \rangle_{\text{max}}$ *cannot* be a fully connected network. In a similar vein, if one wishes to construct a network with $\langle \varphi \rangle > \langle \varphi \rangle_{\text{max}}$ starting from a fully connected network, it is necessary that some connections between nodes are removed, that is, such a network should part from a massively connected to a less connected structure.

Fourthly, $\langle \varphi \rangle_{\text{max}}$ decreases monotonically with N, and $\langle \varphi \rangle_{\text{max}} \to 1/2$ in the thermodynamic limit, i.e., $N \to \infty$.

Finally, and most importantly, the theorem is non-trivial in the sense that one can easily conceive of networks of size N whose global node successes can potentially exceed $\langle \varphi \rangle_{\text{max}}$. For instance, consider the network corresponding to a 'directed ring', where $A_{12} = 1$, $A_{23} = 1, \ldots, A_{(N-1)N} = 1$, $A_{N1} = 1$, and $A_{ij} = 0$ for all other elements of the adjacency matrix. If $w_{ij} = \theta$, then assuming, without loss of generality, that first spike in the network occurs on time step $t = 1$ at node 1, then the spike propagates around the ring indefinitely: at $t = 2$, node 2 spikes; at $t = 3$ node 3 spikes, at $t = N$ node N

spikes, at $t = N + 1$ node 1 spikes, etc. In this case it is easy to see that $\langle \varphi \rangle = 1$, which is greater than $\langle \varphi \rangle_{\max}$ for $N > 2$. Therefore the existence of an upper bound for fully-connected networks stems from some particular property of their topology in combination with the dynamics described in Sect. II.

What is this property of fully-connected networks which places this upper bound on their node success? As alluded to earlier, it is the fact that nodes are frozen for the time step after they spike which gives rise to the upper bound in fully-connected networks. This behaviour gives rise to the phenomenon of *spike jamming* that we mentioned in Sect. III B, and which we describe in detail below.

Consider a single node i firing at time step t in a fully-connected network. For this node to be maximally successful, it must trigger all $N - 1$ of its out-neighbors, i.e., all other nodes in the network, to spike at $t + 1$. Suppose this happens, in which case $\varphi_i(t) = 1$. Consider now one of the nodes $j \neq i$ which spikes at $t + 1$. For j to be maximally successful, all other nodes in the network must spike at $t + 2$. However, on account of refractoriness, this is impossible. To elaborate, at $t + 1$, all nodes except for i, and including j, are spiking. Therefore all these nodes must be frozen at $t + 2$ - they cannot spike at $t + 2$. On the other hand i, which spiked at t, while frozen at $t + 1$, is free to spike at $t + 2$. Hence, at best, only one of the $N - 1$ out-neighbors of j, namely i, can spike at $t + 2$, and therefore at best $\varphi_j(t + 1) = 1/(N - 1)$. For large N, j is clearly very unsuccessful. The same applies for all other nodes which fire at $t + 1$. Hence the result is that, while i is maximally successful, the remaining $N - 1$ nodes are extremely unsuccessful, and hence on average the whole network is unsuccessful during this avalanche - which we assume ends at $t + 2$. This example illustrates the effect which underpins the upper bound for fully-connected networks: if a node i spikes synchronously with one of its out-neighbors, then that out-neighbor is frozen for the next time step, and hence cannot spike on the time step after i spikes, which curtails the potential node success of i, and correspondingly the propagation of spikes throughout the network. Hence we refer to this effect as spike jamming. Note that aforementioned effect occurs in all networks, not just fully-connected networks. However, fully-connected networks are special in that all nodes are out-neighbors of each other, and hence this effect has more potential to curtail the node success in fully-connected networks than in any other network.

IV. DISCUSSION

In this paper we have presented arguments regarding the poor performance (in terms of spiking of individual nodes and their success) of fully-connected networks at criticality showing at the same time that scale-free networks perform much better than any other topology when paired with the small-world property.

Given that the heterogeneous topologies possess exactly the same number of edges, we conclude that scale-free-ness with high degree of small-world-ness is a permutation of edges that allows nodes to be more successful and to be more active in terms of the number of spikes emitted. In particular, we have verified the statement above for the case of in-degree scale-free networks, which feature the presence of *absorbing hubs*. However, real-world networks often comprise a more complex ecosystem in which absorbing hubs and broadcasting hubs coexist in the same network adding another layer of complexity to the dynamics within the system. Moreover, it is often the case that the structure of real-world networks is not static, but they possess mechanisms by which nodes become connected and disconnected over time as well as network growth or shrinkage; features that affect the collective activity in ways that cannot be predicted with the current model.

This leads us to the next consideration. What real system are we describing with the current model? From a certain point of view, the model used here is very limited or simplistic, however a model of integrate-and-fire units can actually be a simplified model of many phenomena in nature. A model of threshold units that accumulate activity from their vicinity and then propagate it when going beyond threshold can be used in principle to model the spread of epidemics, piles of granular matter, the release of energy and relaxation of tectonic plates, the effects of a stock market crash, and the activity of neurons of the brain, among others. Thus, we believe that our model has a broad range of applications in diverse contexts, in which the presence of particular network properties such as the small-world property and long-tailed degree distributions have immediate effects on the dynamics of the system, be it the spread of a disease in a population, the propagation of stimuli on cortical networks, or the spread of rumors and fads within a social network. Moreover, we believe that the introduction of the analysis of the success of a spike can be applied to the situations mentioned above. In other contexts, a spike could be thought of the transmission of an infection among contacts, the death of a species in models of ecosystems, the failure of a power generator in power networks, and even in on-line social networks such as Facebook or Twitter we might regard a spike as the action of writing a *post* or a *tweet*. In all these contexts, the fate of a spike is as relevant to the collective dynamics as is the network topology. Here we have shown that the combination of individual dynamics of nodes and topology determine the success of the spikes that spread across the system.

ACKNOWLEDGMENTS

[1] M. Newman, *Networks: an introduction* (Oxford University Press, Inc., 2010).

[2] D. Watts and S. Strogatz, Nature **393**, 440 (1998).

[3] M. D. Humphries and K. Gurney, PLoS One **3**, e0002051 (2008).

[4] A.-L. Barabási and R. Albert, Science **286**, 509 (1999).

[5] P. Bak, C. Tang, and K. Wiesenfeld, Physical Review A **38**, 364 (1988).

[6] B. Gutenberg and C. F. Richter, Annals of Geophysics **9**, 1 (1956).

[7] V. Frette, K. Christensen, A. Malthe-Sørenssen, J. Feder, T. Jøssang, and P. Meakin, Nature **379**, 49 (1996).

[8] P. Bak, K. Chen, and C. Tang, Physics Letters A **147**, 297 (1990).

[9] C. Eurich, J. Herrmann, and U. Ernst, Physical Review E **66**, 066137 (2002).

[10] P. Bak, *How nature works* (Oxford University Press, Oxford, 1997).

[11] J. Beggs and D. Plenz, the Journal of Neuroscience **23**, 11167 (2003).

[12] T. Petermann, T. Thiagarajan, M. Lebedev, M. Nicolelis, D. Chialvo, and D. Plenz, Proceedings of the National Academy of Sciences **106**, 15921 (2009).

[13] J. Beggs and D. Plenz, The Journal of Neuroscience **24**, 5216 (2004).

[14] A. Levina, J. Herrmann, and T. Geisel, Nature Physics **3**, 857 (2007).

[15] O. Kinouchi and M. Copelli, Nature Physics **2**, 348 (2006).

[16] C. Haldeman and J. Beggs, Physical Review Letters **94**, 58101 (2005).

[17] M. Uhlig, A. Levina, T. Geisel, and J. M. Herrmann, Frontiers in Computational Neuroscience **7** (2013).

[18] N. Bertschinger and T. Natschläger, Neural Computation **16**, 1413 (2004).

[19] J. M. Beggs, Philosophical Transactions of the Royal Society A: Mathematical, Physical and Engineering Sciences **366**, 329 (2008).

[20] M. E. Newman, SIAM review **45**, 167 (2003).

[21] P. Holme and B. J. Kim, Physical Review E **65**, 026107 (2002).

[22] D. B. Larremore, W. L. Shew, and J. G. Restrepo, Physical Review Letters **106**, 058101 (2011).

[23] $\varphi_i(t)$ is undefined if node i does not spike at t.

[24] In obtaining Eqn. (14) we use the fact that if $x \leq a$ and $y \leq b$ then $x + y \leq a + b$.

[25] In obtaining these equations we have used the following rules for manipulating inequalities: if $x \leq a$ then $x + c \leq a + c$ for all c; if $x \leq a$ then $xc \leq ac$ if $c \geq 0$; if $x \leq a$ then $x/c \leq a/c$ if $c > 0$. In applying the second of these rules we used $c = s(t+1)$, which is ≥ 0. In applying the last of these rules we used $c = \sqrt{\mathcal{S}}$, which is > 0.